PHYSICAL REVIEW A VOLUME 43, NUMBER 12 15 JUNE 1991

Generalized hydrodynamic transport in lattice-gas automata

Li-Shi Luo
Center for Nonlinear Studies, Los Alamos National Laboratory, Los Alamos, New Mexico 87545 and School of Physics, Georgia Institute of Technology, Atlanta, Georgia 30332-0430

Hudong Chen
Center for Nonlinear Studies, Los Alamos National Laboratory, Los Alamos, New Mexico 87545 and Department of Physics, Dartmouth College, Hanover, New Hampshire 03755

Shiyi Chen
Center for Nonlinear Studies, Los Alamos National Laboratory, Los Alamos, New Mexico 87545 and Bartol Research Institute, University of Delaware, Newark, Delaware 19716

Gary D. Doolen and Yee-Chun Lee
Center for Nonlinear Studies, Los Alamos National Laboratory, Los Alamos, New Mexico 87545
(Received 14 December 1990)

The generalized hydrodynamics of two-dimensional lattice-gas automata is solved analytically in the linearized Boltzmann approximation. The dependence of the transport coefficients (kinematic viscosity, bulk viscosity, and sound speed) upon wave number $\mathbf{k}$ is obtained analytically. Anisotropy of these coefficients due to the lattice symmetry is studied for the entire range of wave number, $\mathbf{k}$. Boundary effects due to a finite mean free path (Knudsen layer) are analyzed, and accurate comparisons are made with lattice-gas simulations.

Since it was shown theoretically that lattice-gas automata (LGA) can simulate the Navier-Stokes equations,[1-3] lattice-gas automata have been extensively used to study many physical problems in the field of hydrodynamics. Major advantages of the lattice-gas method include its parallel nature and the capability of handling complicated boundary geometries. One significant achievement of the LGA method is the accurate simulation of flow through porous media.[4] Here, we calculate analytically the generalized hydrodynamic LGA transport coefficients using the linearized lattice Boltzmann equation.[2,3,5]

The usual hydrodynamics requires significant modification when the characteristic length scale is the same order as the mean free path. A generalization is required in order to include the wave-number dependence of the transport coefficients in such a way that the constitutive relation is preserved.[6] This generalization produces a nonlocal hydrodynamic response to fluctuations. Generalized hydrodynamics has been studied previously in the context of a hard-sphere fluid.[6,7] The significance of studying generalized hydrodynamics in the context of LGA models is justified by the fact that the LGA method has been used to solve difficult physical problems such as flow through porous media,[4] a situation where generalized hydrodynamics can be important. The purpose of this paper is to present analytic results for the wave-number dependence of transport coefficients in LGA models for the entire range of wave number $\mathbf{k}$ and to examine boundary effects due to a finite mean free path. Previously reported transport coefficients results are valid only in the hydrodynamic limit, $\mathbf{k}=\mathbf{0}$.[2,8] Here, the linearized lattice Boltzmann equation, which is written as an eigenvalue equation valid for all $\mathbf{k}$, is derived and solved analytically.

Before presenting our results, we now briefly describe the lattice-gas model. This many-body lattice-gas system resides on a two-dimensional (2D) hexagonal lattice space $\{\mathbf{x}\}$ with unit lattice constant and with discrete time $t \in \{0,1,2,\ldots\}$. Each particle has unit mass and unit speed. The six possible velocity directions of particles along the links of the hexagonal lattice are:

$$\hat{\mathbf{e}}_\alpha = \cos[(\alpha-1)\pi/3]\hat{\mathbf{x}} + \sin[(\alpha-1)\pi/3]\hat{\mathbf{y}}\,, \qquad \alpha \in \{1,2,\ldots,6\}\,.$$

(Greek indices α, β, ... always run from 1 to 6 unless specified otherwise.) There can be either 1 or 0 particles with the velocity $\hat{\mathbf{e}}_\alpha$ at the same lattice site, $\mathbf{x}$, and time t (exclusion principle). The evolution of the system consists of two steps: collision and streaming. At each time step ($\Delta t = 1$), particle interactions occur through local collisions, i.e., each collision only involves particles at the same site. The collision rules are designed to conserve the exact particle number, momentum, and kinetic energy. After collision, particles move in the direction of their velocities to adjacent sites.

The evolution of the Frisch-Hasslacher-Pomeau (FHP) lattice-gas system is completely determined by the microscopic equation

$$N_\alpha(\mathbf{x}+\hat{\mathbf{e}}_\alpha, t+1) = N_\alpha(\mathbf{x},t) + C_\alpha(N)\,, \tag{1}$$

where N denotes all $N_\alpha(\mathbf{x},t)$ and the Boolean function

$$C_\alpha(N) = \sum_{s,s'} (s'_\alpha - s_\alpha)\xi_{ss'} \prod_\beta N_\beta^{s_\beta}(\mathbf{x},t)[1-N_\beta(\mathbf{x},t)]^{(1-s_\beta)} \tag{2}$$

represents creation or annihilation of $N_\alpha(\mathbf{x},t)$ due to collisions for all possible incoming configuration s and outgoing configuration s′ at a given site x. The quantity $\xi_{ss'}$ is a random Boolean number in time and space, satisfying the normalization condition

$$\sum_{s'}\xi_{ss'}=1 \quad \forall s$$

and the conservation conditions

$$\sum_{\alpha}(s'_\alpha-s_\alpha)\xi_{ss'}h_\alpha=0\,,$$

where h_α is any linear combination of 1, $(\hat{\mathbf{e}}_\alpha)_x\equiv\cos[(\alpha-1)\pi/3]$ and $(\hat{\mathbf{e}}_\alpha)_y\equiv\sin[(\alpha-1)\pi/3]$. The average value of $\xi_{ss'}$, $A_{ss'}=\langle\xi_{ss'}\rangle$, defines a transition probability from state s to s′, for any arbitrary s and s′. Moreover, $\xi_{ss'}$ has rotational symmetry, i.e., for any s and s′, $\xi_{ss'}$ is invariant if states s and s′ are both subjected to simultaneous proper or improper rotations. Also, different values for $A_{ss'}$ produce different values for the transport coefficients, but their qualitative behavior will not change.

The ensemble average of Eq. (1) using the random-phase approximation yields the lattice Boltzmann equation:[5]

$$f_\alpha(\mathbf{x}+\hat{\mathbf{e}}_\alpha,t+1)=f_\alpha(\mathbf{x},t)+\Omega_\alpha(f)\,, \tag{3}$$

where $f_\alpha(\mathbf{x},t)$ is the single-particle distribution function, and f denotes all of $f_\alpha(\mathbf{x},t)$. The operator Ω_α is equal to C_α if N_β and $\xi_{ss'}$ are replaced by f_β and $A_{ss'}$, respectively, in Eq. (2). The particle-number density $n(\mathbf{x},t)$ and momentum density $\mathbf{p}(\mathbf{x},t)$ are related to $f_\alpha(\mathbf{x},t)$ by $n(\mathbf{x},t)=\sum_\alpha f_\alpha(\mathbf{x},t)$, and $\mathbf{p}(\mathbf{x},t)=\sum_\alpha\hat{\mathbf{e}}_\alpha f_\alpha(\mathbf{x},t)$, respectively. With the random-phase approximation, which neglects the instantaneous correlations between particles involved in a collision process, one can show that the single-particle distribution function $f_\alpha(\mathbf{x},t)$ obeys the Fermi-Dirac distribution.[2,3]

Assume that $f_\alpha(\mathbf{x},t)=d[1+\phi_\alpha(\mathbf{x},t)]$ with $|\phi_\alpha|\ll1$, where d is the equilibrium density for zero mean velocity. We can linearize Eq. (3) to obtain

$$\phi_\alpha(\mathbf{x}+\hat{\mathbf{e}}_\alpha,t+1)=\phi_\alpha(\mathbf{x},t)+\sum_\beta\Omega^{(1)}_{\alpha\beta}\phi_\beta(\mathbf{x},t)\,, \tag{4}$$

where the linearized collision operator $\Omega^{(1)}_{\alpha\beta}$ is the 6×6 real circulant matrix:[9]

$$\Omega^{(1)}_{\alpha\beta}=-\tfrac{1}{2}\sum_{s,s'}(s'_\alpha-s_\alpha)(s'_\beta-s_\beta)A_{ss'}d^{\sigma_s-1}(1-d)^{5-\sigma_s}\,, \tag{5}$$

where $\sigma_s=\sum_\alpha s_\alpha$ is the number of particles in configuration s. Note that $\Omega^{(1)}$ only depends on the equilibrium density d for a given set of collision rules. The Fourier transform of Eq. (4) is

$$\phi_\alpha(\mathbf{k},t+1)=e^{-i\mathbf{k}\cdot\hat{\mathbf{e}}_\alpha}\sum_\beta(\delta_{\alpha\beta}+\Omega^{(1)}_{\alpha\beta})\phi_\beta(\mathbf{k},t)\,. \tag{6}$$

This can be written in vector form

$$|\phi(\mathbf{k},t+1)\rangle=H(\mathbf{k})|\phi(\mathbf{k},t)\rangle\,, \tag{7}$$

where the component of the fluctuation vector $\langle\alpha|\phi(\mathbf{k},t)\rangle$ is $\phi_\alpha(\mathbf{k},t)$. The matrix $H(\mathbf{k})=D(\mathbf{k})H(0)$, where $H(0)=I+\Omega^{(1)}$, is the evolution operator. The diagonal matrix $D(\mathbf{k})=\mathrm{diag}(\exp(-i\mathbf{k}\cdot\hat{\mathbf{e}}_1),\exp(-i\mathbf{k}\cdot\hat{\mathbf{e}}_2),\ldots,\exp(-i\mathbf{k}\cdot\hat{\mathbf{e}}_6))$ is the displacement operator.

In general, the eigenvalue problem for $H(\mathbf{k})$ cannot be solved analytically except for special cases, whereas that for $H(0)$ can be trivially solved because $H(0)$ is a circulant matrix. The matrix $H(0)$ has three unit eigenvalues corresponding to the three hydrodynamic modes, i.e., the corresponding eigenvectors are associated with the conserved quantities of the system. $H(0)$ also has three non-unit eigenvalues corresponding to three kinetic modes. It can be rigorously shown that these modes can be analytically continued to the $\mathbf{k}\neq0$ region [as indicated by Eq. (14) later]. Although our procedure is general, we illustrate it using the six-bit collision-saturated nondeterministic FHP model[2] in what follows. In this case,

$$H(0)=\mathrm{circ}(p_1,p_2,p_3,p_4,p_3,p_2)\,,$$

with $p_1=1-\tilde{d}(1+3\tilde{d})$, $p_2=\tilde{d}(1+4\tilde{d})/2$, $p_3=\tilde{d}/2$, $p_4=-\tilde{d}(1+\tilde{d})$, and $\tilde{d}\equiv d(1-d)$. The eigenvalues of $H(0)$ are $\lambda_{1,2,6}=1$, $\lambda_{3,5}=1-3\tilde{d}(1+2\tilde{d})$, and $\lambda_4=1-6\tilde{d}^2$. The eigenvectors of $H(0)$ with unit eigenvalue are

$$|n\rangle=\frac{1}{\sqrt{6}}\begin{bmatrix}1\\1\\1\\1\\1\\1\end{bmatrix},\quad |p_{x0}\rangle=\frac{1}{2\sqrt{3}}\begin{bmatrix}2\\1\\-1\\-2\\-1\\1\end{bmatrix},\quad\text{and}\quad |p_{y0}\rangle=\frac{1}{2}\begin{bmatrix}0\\1\\1\\0\\-1\\-1\end{bmatrix}, \tag{8}$$

which are the density, x-momentum, and y-momentum modes, respectively. Denoting θ as the angle between $\mathbf{k}$ and $\hat{\mathbf{e}}_1$ $(=\hat{\mathbf{x}})$, $|u_t(\mathbf{k})\rangle$, and $|u_\pm(\mathbf{k})\rangle$ as the generalized hydrodynamic eigenvectors, the zeroth order (in $\mathbf{k}$) hydrodynamic eigenvectors of $H(\mathbf{k})$ are

$$|u_t(0)\rangle=\cos\theta|p_{y0}\rangle-\sin\theta|p_{x0}\rangle=|p_t\rangle\,, \tag{9}$$

$$\begin{aligned}|u_\pm(0)\rangle&=\frac{1}{\sqrt{2}}[|n\rangle\pm(\cos\theta|p_{x0}\rangle+\sin\theta|p_{y0}\rangle)]\\&=\frac{1}{\sqrt{2}}(|n\rangle\pm|p_l\rangle)\,,\end{aligned} \tag{10}$$

where $|p_t\rangle$ and $|p_l\rangle$ denote the transverse and longitudinal momentum with respect to $\mathbf{k}$. If we let $\phi_t(\mathbf{k},t)=\langle u_t(\mathbf{k})|\phi(\mathbf{k},t)\rangle$ and $\phi_\pm(\mathbf{k},t)=\langle u_\pm(\mathbf{k})|\phi(\mathbf{k},t)\rangle$, then the generalized hydrodynamic equations for the linearized lattice Boltzmann equation are

$$\phi_t(\mathbf{k},t+1)=z_t(\mathbf{k})\phi_t(\mathbf{k},t)=e^{(t+1)\ln z_t}\phi_t(\mathbf{k},0)\,, \tag{11}$$

$$\phi_\pm(\mathbf{k},t+1)=z_\pm(\mathbf{k})\phi_\pm(\mathbf{k},t)=e^{(t+1)\ln z_\pm}\phi_\pm(\mathbf{k},0)\,, \tag{12}$$

and the generalized hydrodynamic transport coefficients are defined in analogy to their definitions in hydrodynamics:[6]

$$\begin{aligned}\nu(\mathbf{k})&=-\frac{\ln(z_t(\mathbf{k}))}{k^2}\,,\\ \tfrac{1}{2}\nu(\mathbf{k})+\eta(\mathbf{k})&=-\frac{\mathrm{Re}[\ln(z_\pm(\mathbf{k}))]}{k^2}\,,\\ c_s(\mathbf{k})&=\mp\frac{\mathrm{Im}[\ln(z_\pm(\mathbf{k}))]}{k}\,,\end{aligned} \tag{13}$$

where ν, η, and c_s are the kinematic viscosity, the bulk viscosity, and the sound speed, respectively. By expanding $D(\mathbf{k})$ in $\mathbf{k}$, i.e., $D(\mathbf{k})=\sum_n(-ik)^n P^n(\theta)/n!$ with

$$P(\theta)=\text{diag}[\cos\theta,\cos(\theta-\pi/3),\ldots,\cos(\theta+\pi/3)],$$

the coefficients of perturbation expansions for the eigenvalues can be calculated. The coefficients in perturbation expansions for the transport coefficients are just the cumulants[10] of the corresponding eigenvalues. As an example, the first few coefficients in perturbation expansions for $z_t(\mathbf{k})$ and the kinematic viscosity $\nu(\mathbf{k})$ are given as follows:

$$z_t(\mathbf{k})=1-z_t^{(2)}k^2+z_t^{(4)}k^4+\ldots$$

where

$$z_t^{(2)}=(1+\lambda_3)/8(1-\lambda_3),$$

$$z_t^{(4)}=[z_t^{(2)}/48(1-\lambda_4)(1-\lambda_3)^2]\times[2(1+2\lambda_4-2\lambda_3+2\lambda_4\lambda_3-5\lambda_3^2+2\lambda_4\lambda_3^2)-\cos(6\theta)(1-\lambda_3)(1+5\lambda_3+5\lambda_4+\lambda_3\lambda_4)],$$

$$\nu(\mathbf{k})=\nu_0-\nu_2k^2+\ldots,$$

where $\nu_0=z_t^{(2)}$ and $\nu_2=(z_t^{(2)})^2/2-z_t^{(4)}$. The zeroth order (in $\mathbf{k}$) results of the transport coefficients obtained by this perturbative method are identical to the previous results.[2,3]

In the case of $\theta=0$ or $\theta=\pi/6$, the eigenvalues of $H(\mathbf{k})$ are obtained analytically for arbitrary k. For $\theta=0$, $H(\mathbf{k})$ can be decomposed into the direct sum of a 2×2 and a 4×4 matrix. For $\theta=\pi/6$, $H(\mathbf{k})$ becomes a direct sum of two 3×3 matrices. Therefore the eigenvalues are roots of quadratic, quartic, or cubic algebraic polynomials. The decomposition of $H(\mathbf{k})$ along the special directions $\theta=0$ and $\theta=\pi/6$ is consequence of the fact that the collision operator Ω_α is invariant under the complete lattice symmetry group.[3] This decomposition is also applicable to other FHP 2D models.

For $\theta=0$,

$$z_t(\mathbf{k})=\tfrac{1}{2}(1+\lambda_3)\cos(\tfrac{1}{2}k)+\tfrac{1}{2}\sqrt{(1+\lambda_3)^2\cos^2(\tfrac{1}{2}k)-4\lambda_3}. \quad (14)$$

The kinematic viscosity possesses an imaginary part between the two branch points which satisfy $(1+\lambda_3)^2\times\cos^2(k/2)-4\lambda_3=0$. As k increases from 0 to the first branch point, $z_t(\mathbf{k})$ and the eigenvalue of the kinetic mode coupled by the quadratic equation collide with each other. Then both of them become complex conjugates until they collide again at the second branch point. After the second collision they separate along the real axis of the z plane. Numerical results indicate that a similar situation occurs when $0<\theta<\pi/6$ for the transverse mode. However, when $\theta=\pi/6$ the kinematic viscosity has no imaginary part in the physical region $(0<d<1)$ of the k-d plane. The fact that $z_t(\mathbf{k})$ can be complex indicates that the relaxation of the transverse momentum can be oscillatory. In the limit $d\to0$, $z_t(\mathbf{k})\to e^{ik/2}$. This suggests that oscillations in relaxations of the transverse momentum are related to the free streaming of particles (a ballistic effect).

Plots of the wave-number dependence of the kinematic viscosity ν, the bulk viscosity η, and the sound speed c_s for density $d=0.2$ and $\theta=0$, $\pi/12$, and $\pi/6$ are shown in Figs. 1(a)–1(c). For $\theta=\pi/12$, results are obtained by calculating the eigenvalues of $H(\mathbf{k})$ directly. We also calculated $\nu(\mathbf{k})$ and $c_s(\mathbf{k})$ by perturbation expansion for $\theta=\pi/12$. The eighth order perturbative result of $\nu(\mathbf{k})$ agrees with the exact result for $k\leq0.5$; for $c_s(\mathbf{k})$, results agree when $k\leq0.2$. One can clearly see that these transport coefficients are highly anisotropic even for moderate values of k. This fact indicates that in LGA simulations, a large number of cells must be averaged over in order to overcome the anisotropy.

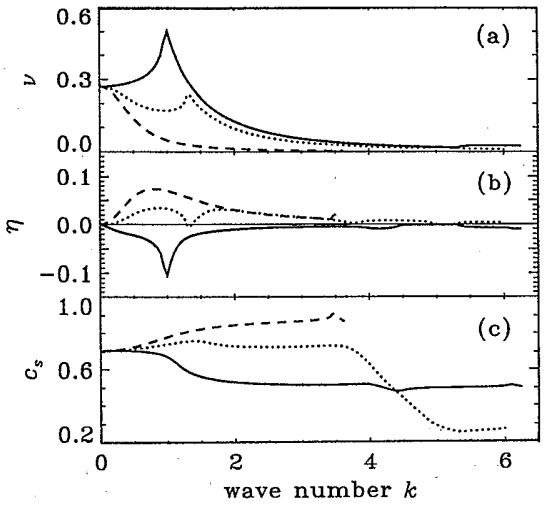

FIG. 1. Kinematic viscosity $\nu(\mathbf{k})$, bulk viscosity $\eta(\mathbf{k})$, and sound speed $c_s(\mathbf{k})$ vs $\mathbf{k}$ for density equal to 0.2, and $\theta=0$ (solid line), $\pi/12$ (dotted line), and $\pi/6$ (dashed line). (a) $\nu(\mathbf{k})$ vs $\mathbf{k}$; (b) $\eta(\mathbf{k})$ vs $\mathbf{k}$; (c) $c_s(\mathbf{k})$ vs $\mathbf{k}$.

In Fig. 2, the analytic result and LGA simulations of c_s are compared for the direction $\theta=\pi/6$. Simulation results confirm the prediction of the analytic result that c_s increases as k increases along the direction $\theta=\pi/6$.

In Fig. 3, the momentum profile of forced flow between parallel plates (Poiseuille flow)[11] from our analysis and LGA simulations are compared. The geometric arrangement and forcing rules of the simulation are the same as

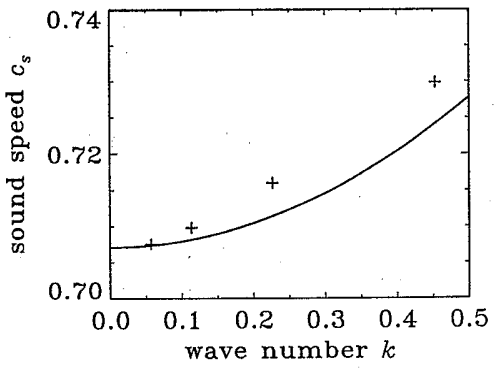

FIG. 2. Sound speed $c_s(\mathbf{k})$ vs k for density $d=0.2$ and $\theta=\pi/6$. The analytic result is represented by the solid line and the LGA simulations by "+". The relative differences between the LGA simulation and the analytic result are less than 1%.

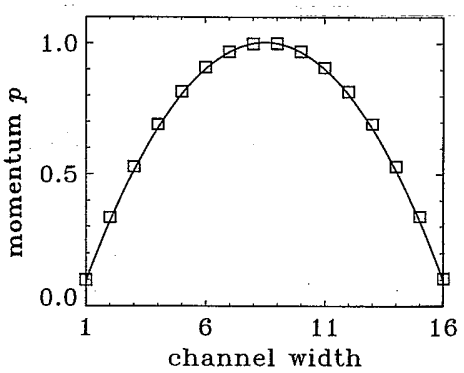

FIG. 3. Momentum profile of Poiseuille flow for density $d=0.2$ and a channel width of 16 lattice sites. To obtain a steady state, 10^6 time iterations were run before the average. The momentum p_x is averaged over L_y and over 2×10^6 time iterations. The analytic result [Eq. (16)] is represented by the solid line and the LGA simulation by "□". The graph is rescaled so that $p_{\max}=1$. Note the agreement for the nonzero momentum at the walls due to the finite mean free path. The simulation was run on a Cray-YMP computer, with $F_0=1.0641\times10^{-3}$.

in Ref. 11: plates are arranged parallel to a velocity direction, and periodic boundary conditions are applied. The system size is $L_x\times L_y=512\times32$, where L_y is twice the channel width. The forcing is a square-wave function between plates: it is of uniform magnitude on sites $1\le y\le16$ and of opposite uniform magnitude on sites $17\le y\le32$.

Assume Eq. (4) with a term of the square wave forcing along the $\hat{\mathbf{x}}$ direction, which is parallel to the boundaries. Let $\mathbf{k}$ be along the $\hat{\mathbf{y}}$ direction and assume a steady state, i.e., $|\phi(\mathbf{k},t+1)\rangle=|\phi(\mathbf{k},t)\rangle$. Then the discrete Fourier transform of the momentum profile is

$$p_x(y)=\frac{F_0}{2N}\sum_{k=1}^{N}\left[a+\frac{6b}{\sin^2[\sqrt{3}(2k-1)\pi/4N]}\right]\times\frac{4\sin[(2k-1)\pi y/N]}{2N(2k-1)\pi},\quad 0\le y\le 2N-1, \tag{15}$$

where F_0 is the magnitude of forcing, $N=L_y/2$,

$$a=(2-3\tilde{d}-15\tilde{d}^2)/[3\tilde{d}^2(2-3\tilde{d}-6\tilde{d}^2)]$$

and

$$b=3\tilde{d}(1+2\tilde{d})/4(2-3\tilde{d}-6\tilde{d}^2).$$

In the thermodynamic limit ($N\to\infty$, $d\to0$, and $2Nd\to d_0=$const), the following parabolic profile for $p_x(y)$ is obtained:

$$\bar{p}_x(\bar{y})=\lim_{N\to\infty,d\to0}p_x(y)=\begin{cases}F_0[4\bar{b}\bar{y}(1-\bar{y})+\bar{a}], & 0\le\bar{y}<1,\\ F_0[4\bar{b}(\bar{y}-1)(\bar{y}-2)-\bar{a}], & 1\le\bar{y}<2,\end{cases} \tag{16}$$

where $\bar{a}=1/(3d_0^2)$, $\bar{b}=3d_0/8$, and $\bar{y}=y/N$. We can rewrite $\bar{a}=2\bar{l}$, where $\bar{l}$ is the mean free path in the limit. Therefore, the discontinuity of the momentum profiles, which presents the slip velocity at the walls,[12] is proportional to the mean free path in the limit. Note that in Fig. 3 the discontinuity of the momentum profiles at the boundaries (the slip momentum) is accurately predicted by the analysis. This phenomenon is a manifestation of existence of a Knudsen layer.[12,13]

In conclusion, we have obtained an analytical solution of the linearized lattice Boltzmann equation. We have quantitatively analyzed boundary effects due to a finite mean free path (Knudsen layer) and anisotropy effects due to the lattice symmetry, and find agreement with LGA simulations.

We are very grateful to Dr. H. A. Rose for his valuable suggestions. We thank Professor David Levermore for many helpful conversations and for showing us Ref. 13 before publication, and we thank Dr. E. Y. Loh, Jr. for guidance in the use of the Connection Machine. One of the authors (S.C.) would like to acknowledge the support from the NASA Innovative Research Program under Grant No. NAGW-1648. This work is supported in part by the U.S. Department of Energy and by the Defense Advanced Research Project Agency Grant No. DPP88-50.

[1]U. Frisch, B. Hasslacher, and Y. Pomeau, Phys. Rev. Lett. **56**, 1505 (1986).
[2]U. Frisch *et al.*, Complex Syst. **1**, 649 (1987).
[3]S. Wolfram, J. Stat. Phys. **45**, 471 (1986).
[4]S. Chen *et al.*, Physica D **47**, 72 (1991); D. H. Rothman, Geophysics **53**, 509 (1988).
[5]G. R. McNamara and G. Zanetti, Phys. Rev. Lett. **61**, 2332 (1988).
[6]B. J. Alder and W. E. Alley, Phys. Today **37** (1), 56 (1984).
[7]I. M. de Schepper and E. G. D. Cohen, J. Stat. Phys. **27**, 223 (1982).
[8]M. Hénon, Complex Syst. **1**, 763 (1987).
[9]P. J. Davis, *Circulant Matrices* (Wiley, New York, 1979).
[10]G. A. Korn and T. M. Korn, *Mathematical Handbook for Scientists and Engineers,* 2nd ed. (McGraw-Hill, New York, 1968), pp. 600-601.
[11]L. P. Kadanoff, G. R. McNamara, and G. Zanetti, Complex Syst. **1**, 791 (1987).
[12]D. K. Bhattacharya and G. C. Lie, Phys. Rev. Lett. **62**, 897 (1989); G. Mo and F. Rosenberger, Phys. Rev. A **42**, 4688 (1990).
[13]R. Cornubert, D. d'Humiéres, and D. Levermore, Physica D **47**, 241 (1991).